Photoelectron imaging of tetrahydrofuran cluster anions $(THF)_n^-$ $(1 \leq n \leq 100)$

Ryan M. Young,[1] Margaret A. Yandell,[1] Markus Niemeyer,[2] and Daniel M. Neumark[1,3,a)]
[1]*Department of Chemistry, University of California, Berkeley, California 94720, USA*
[2]*Technische Universität Berlin, IOAP, EW 3-1, Hardenbergstraße 36, D-10623 Berlin, Germany*
[3]*Chemical Sciences Division, Lawrence Berkeley National Laboratory, Berkeley, California 94720, USA*

(Received 27 July 2010; accepted 24 August 2010; published online 20 October 2010)

Anionic tetrahydrofuran clusters $(THF)_n^-$ $(1 \leq n \leq 100)$ are studied with photoelectron imaging as gas-phase precursors for electrons solvated in THF. Photoelectron spectra of clusters up to $n=5$ show two peaks, one of which is attributed to a solvated open chain radical anion and the other to the closed THF ring. At $n=6$, the spectra change shape abruptly, which become more characteristic of $(THF)_n^-$ clusters containing solvated electrons. From $n=6-100$, the vertical detachment energies (VDEs) of these solvated electron clusters increase from 1.96 to 2.71 eV, scaling linearly with $n^{-1/3}$. For fully deuterated $(THF\text{-}d8)_n^-$ clusters, the apparent transition to a solvated electron cluster is delayed to $n=11$. Extrapolation of the VDEs to infinite cluster size yields a value of 3.10 eV for the bulk photoelectric threshold. The relatively large VDEs at onset and small stabilization with increasing cluster size compared to other solvated electron clusters may reflect the tendency of the bulk solvent to form preexisting voids that can readily solvate a free electron. © *2010 American Institute of Physics*. [doi:10.1063/1.3489686]

I. INTRODUCTION

The solvated electron has long been of interest to physical scientists as it plays a key role in diverse phenomena including quantum interactions in condensed phases,[1,2] the atmospheric chemistry of aerosols,[3] and low-energy radiation damage of DNA.[4] Solvated electrons are the simplest quantum mechanical solute, and studies of electron solvation phenomena probe fundamental aspects of this solute-solvent interaction.[1,5,6] While solvated electrons are most frequently studied in aqueous solution,[1,7] they exist in a multitude of organic and inorganic solvents.[8–10] Experiments in solution have been complemented by studies of gas phase water cluster anions[11–14] and clusters comprising electrons bound to other solvent molecules such as acetonitrile,[15,16] benzene,[17] methanol,[18,19] and formamide.[20] The cluster work has yielded a great deal of insight into how excess electrons interact with small numbers of molecules and how this interaction evolves toward that of the bulk solution as the number of solvent molecules increases.[21,22] In this paper, we report experiments in which tetrahydrofuran cluster anions $(THF)_n^-$ are observed for the first time and are characterized using photoelectron spectroscopy in order to study the solvation of excess electrons in a weakly polar medium.

The interaction of THF with electrons has been studied in both gas phase and condensed phase environments. The gas phase experiments and accompanying theory have considered electron scattering total and differential cross sections,[23–25] the ion mass distribution resulting from dissociative electron attachment,[26,27] and the electron energy loss spectrum.[28] These investigations are motivated by the notion that THF is a model system for the ribose ring in nucleic acids, and that electron scattering from THF can thus provide insight into the radiation damage induced in DNA by low energy electrons.

More relevant to the work reported here are the extensive experimental and theoretical studies by Schwartz[29–33] and Ruhman[34] on the spectroscopy and dynamics of solvated electrons in liquid THF. Most of these experiments have focused on forming the sodide (Na^-) anion in THF, ejecting an electron into the solvent by excitation of the charge-transfer-to-solvent (CTTS) transition with a femtosecond laser pulse, and monitoring the ensuing dynamics with 1 or 2 different fs probe pulses. The CTTS transition for the sodide anion, which is easily formed in THF, is centered around 780 nm, which makes it readily accessible to Ti:sapphire laser excitation, while the absorption spectrum of solvated electrons in THF peaks around 2000 nm and is hence well-separated from the CTTS transition. The overall experimental arrangement is similar to that used for the CTTS excitation of halide anions in aqueous solution,[35] but both the CTTS and solvated electron transitions are substantially redshifted in the sodide/THF experiments.

Simulations by Schwartz[30,31] and neutron diffraction experiments by Soper[36] have shown that liquid THF has unusual aspects that can significantly affect electron solvation. Specifically, there appear to be preexisting voids with diameters in the range of 2.5–5 Å within the solvent network. Moreover, the simulations and experiments suggest that these empty spaces are partially positively polarized and can therefore act as traps for solvated electrons, which allow for solvation with little nuclear rearrangement. The presence of these voids has been invoked by Sanche[37] to explain the very high trapping efficiency of low energy electrons by thin films

a)Author to whom correspondence should be addressed. Electronic mail: dneumark@berkeley.edu.

of THF. This picture of electron solvation in THF is in sharp contrast to the widely accepted cavity model for electrons in water,[1] in which the electrons have to push water molecules aside to form a cavity with a radius of ~2.5 Å. Moreover, in water, the low-lying excited states of the hydrated electron are quite localized with respect to its ground state, whereas in THF the excited states have amplitude not only in the preformed cavity in which the electron originally resides but also in nearby unoccupied cavities.[30]

The condensed phase results on electrons in THF raise the question of how the properties of liquid THF might manifest themselves in negatively charged cluster anions. Specifically, it is of considerable interest to determine if the tendency of bulk THF to form preexisting voids that can readily accommodate excess electrons translates into measurable trends in the energetics, spectroscopy, and dynamics of $(THF)_n^-$ clusters. As a first step in this direction, we report the first observation of $(THF)_n^-$ clusters in the gas phase and their one-photon photoelectron spectra. The experiments yield vertical detachment energies (VDEs) for clusters up to $n=100$, and provide evidence that a minimum of six THF molecules is needed to form a "solvated electron cluster."

II. EXPERIMENTAL

The experiments were performed on our time-resolved anion photoelectron imaging apparatus,[38] although the work described here did not involve any explicitly time-resolved measurements. Briefly, argon gas at 20 psig was flowed over THF at room temperature, where it picked up the vapor over the liquid and was coexpanded into a vacuum chamber through a pulsed solenoid valve[39] operating at 100 Hz. Collisions within the expansion cooled the gas and induced clustering of the THF molecules. The ionization occurred via secondary attachment of electrons from a ring-electrode ionizer that intercepted the gas during expansion. The resulting ions were then injected perpendicularly into a Wiley–McLaren time-of-flight mass spectrometer.[40] An electrostatic switch pulsed at the appropriate delay time acted as a mass gate, allowing ions of the desired mass to pass into the interaction region where a laser pulse photodetached the electrons. Mass spectra were collected with a retractable microchannel plate (MCP) detector within the interaction region and recorded on a digital oscilloscope (Tektronix DPO3034).

The photodetachment light pulses were generated by a commercial Ti:sapphire oscillator and multipass chirped pulse amplifier (KM Laboratories Griffin oscillator, Dragon amplifier) yielding 30 fs pulses at 790 nm (1.57 eV). A fraction of this light was then directed into a 29.2° beta barium borate (BBO) crystal to generate the second harmonic at 395 nm (3.14 eV, 100 μJ/pulse at 600 Hz) that was used to photodetach the anions.

The resulting photoelectrons were accelerated, detected, and analyzed using velocity map imaging (VMI),[41] yielding their kinetic energy and angular distributions. The imaging detector comprised a chevron-mounted dual MCP stack coupled to a phosphor screen. 12-bit images were recorded at 30 frames per second with a charge-coupled devide (CCD) camera. Images were integrated over ~10^5 laser pulses with 5–10 photoelectrons/pulse. The resulting images were then four-way symmetrized to account for detector inhomogeneities and transformed with the basis-set expansion method (BASEX),[42] recovering the full velocity distribution. The VMI/camera system was calibrated by photodetachment of O_2^- anions[43] with 395 nm laser pulses.

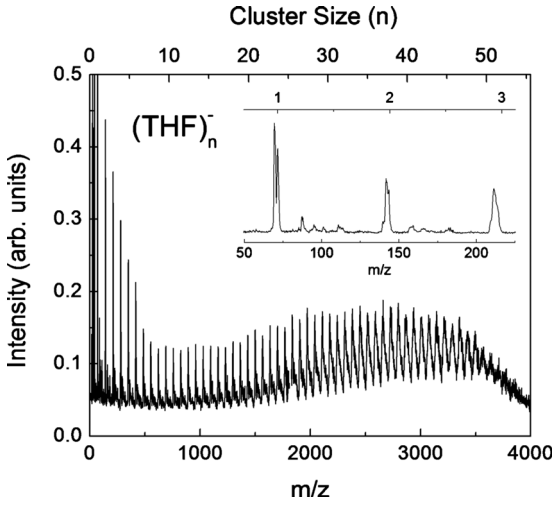

FIG. 1. Time-of-Flight mass spectrum of $(THF)_n^-$ cluster anions. Inset shows mass spectrum in the range $n=1-3$. The first peak is split by the presence of (1,2)-*s*-$C_4H_7O^-$ at $m/z=71$. Cluster number assignments are assigned based on flight times relative to this peak.

Angular integration of the transformed images yielded the electron speed distribution, from which one derives the distribution of electron kinetic energies (eKE) and electron binding energies (eBE), where eBE=hν−eKE. Single photon photoelectron angular distributions (PADs) were recovered by fitting the transformed images to[44,45]

$$I(\theta,\mathrm{eKE};n)=\frac{\sigma_{\mathrm{total}}}{4\pi}[1+\beta(\mathrm{eKE};n)P_2(\cos\,\theta)]. \quad (1)$$

Here θ is the angle between the ejected photoelectron wave and the laser polarization, σ_{total} is the total photodetachment cross section, n is the cluster size, and $P_2(\cos\,\theta)$ is the second-order Legendre polynomial. The anisotropy parameter β, which lies between 2 and −1, specifies the nature of the PAD at each value of the eKE.

To aid in assigning the photoelectron spectra, electronic structure calculations were performed using density functional theory (DFT) with the B3LYP functional and the 6-311++G** basis set for correlation in the GAUSSIAN 03 (Ref. 46) software package. The VDEs for species of interest were computed as the difference in absolute energies between anion and neutral molecules frozen at the optimized anion geometry.

III. RESULTS AND ANALYSIS

A. Mass spectrum

A representative anion mass spectrum is shown in Fig. 1. Nearly all peaks in the spectrum fit a $(THF)_n^-$ cluster distribution beginning at $n=1$ ($m/z=72$), with single-size resolution extending to $n\sim55$, beyond which clusters can still be isolated to within $\Delta m/m\sim1\%$ using the calibration method

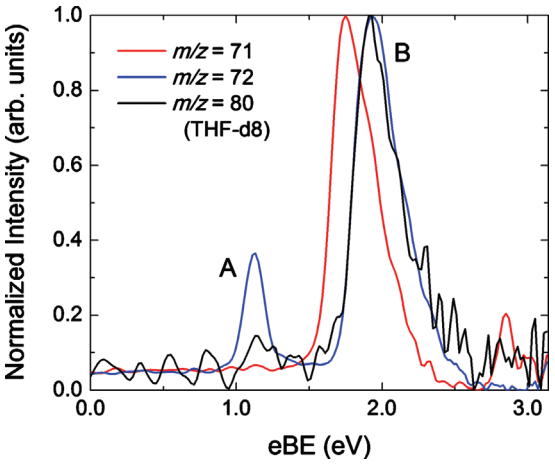

FIG. 2. Photoelectron spectrum of $m/z=71$ (red), $m/z=72$ (blue), and $m/z=80$ (black) taken at a photon energy of 3.14 eV. The curve for $m/z=72$ shows two peaks: feature A at 1.12 eV and feature B at 1.87 eV.

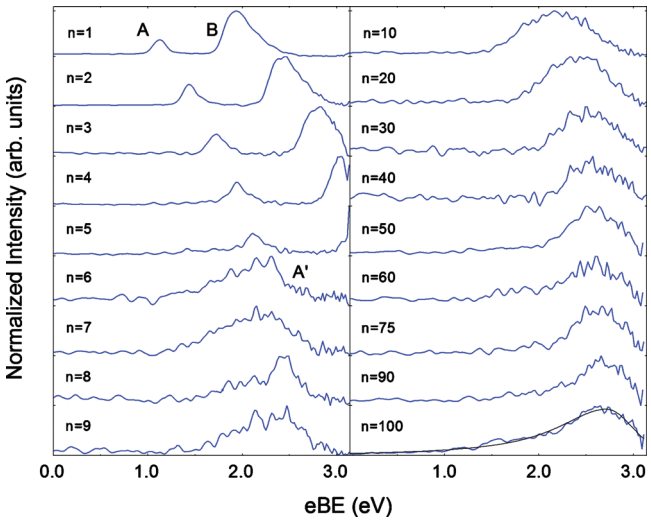

FIG. 3. Selected normalized photoelectron spectra of $(THF)_n^-$ cluster anions taken with $h\nu=3.14$ eV from $n=1$ to 100. Features A and B from Fig. 2 are seen through $n=5$. Starting at $n=6$, the single remaining feature is relabeled as feature A′. A Gaussian–Lorentzian profile (black curve) is imposed on $n=100$ for comparison of the fit function.

described previously.[13,18] The inset of Fig. 1 shows the first few peaks of the mass distribution. The signal near $n=1$ is split into two peaks with $m/z=71$ and 72, both of which are discussed in more detail below. Ions generated from fully deuterated THF-d8 show the analogous pattern of peaks (with different peak separations), while ions generated from a different constitutional isomer of C_4H_8O, butyraldehyde, yield a very different mass spectrum. These additional measurements support assignment of the main pattern of peaks in Fig. 1 to $(THF)_n^-$ clusters.

B. Photoelectron spectra

Figure 2 shows the photoelectron (PE) spectrum of the anion at $m/z=72$ (blue curve), where it is compared to that of the anion at $m/z=71$ (red curve). The PE spectrum of the $m/z=71$ peak corresponds to that of the *sec*-butyraldehyde enolate $[(1,2)\text{-}s\text{-}C_4H_7O^-]$ as observed by Continetti *et al.*[47] The spectrum for $m/z=72$ has two clear peaks at VDE $=1.12$ eV (feature A) and VDE$=1.87$ eV (feature B). Feature A is structureless and narrow, with a full-width at half-maximum (FWHM) of 130 meV, larger than the experimental resolution of 45 meV set by the bandwidth of the femtosecond laser pulse. The anisotropy parameter β associated with this feature is 1.60 ± 0.10, signifying that this feature originates from a highly symmetric *s*-like molecular orbital. The shape of feature B suggests underlying vibrational structure, and its PAD is isotropic, with $\beta\sim0$. The PE spectrum of the anion with $m/z=80$ from THF-d8 is also shown in Fig. 2; feature B is the same in this spectrum, but feature A is much less intense.

Figure 3 shows normalized photoelectron spectra for selected members of the $(THF)_n^-$ progression from $n=1$ to $n=100$. The two sharp features seen in Fig. 2, are apparent up to $n=5$, and progressively shift to higher binding energies with increasing cluster size. By $n=5$, feature B is barely accessible at our photodetachment energy of 3.14 eV. The relative intensities of both features remain constant over $n=1-5$.

At $n=6$, the PE spectral shape changes dramatically compared to the smaller clusters, becoming markedly broader and less symmetric. From $n=6-100$, the VDEs increase monotonically from 1.96 to 2.71 eV; VDEs at each cluster size are determined by fitting the binding energy spectrum to a Gaussian distribution peaked at the VDE with width w_G (FWHM$=2w_G\sqrt{\ln 2}$). For larger cluster sizes ($n\geq50$), the asymmetry becomes more pronounced and the spectra are best fit to a Gaussian–Lorentzian profile[21] where the low and high binding energy sides of the peak energy (VDE_n) are fit by a Lorentzian with width w_L and a Gaussian with width w_G, respectively,

$$I(\mathrm{eBE};n) = \begin{cases} I_0 + A\left[\dfrac{w_L^2}{(\mathrm{eBE}-\mathrm{VDE}_n)^2+w_L^2}\right] & \mathrm{eBE} < \mathrm{VDE}_n \\ I_0 + Ae^{-(\mathrm{eBE}-\mathrm{VDE}_n)^2/w_G^2} & \mathrm{eBE} \geq \mathrm{VDE}_n, \end{cases} \quad (2)$$

(FWHM$=w_G\sqrt{\ln 2}+w_L$). A fit to Eq. (2) (black curve) is superimposed on the data for $n=100$ in Fig. 3 to demonstrate the appropriateness of this choice of fit function for this size regime.

Figure 4 shows peak widths and photoelectron anisotropy parameters β for feature A in anions with $n=1-5$ and for the single peak seen for the larger clusters. The peak width more than doubles going from $n=5$ to $n=6$, after which it remains relatively constant. Similarly, β shows a large drop from $n=5$ to 6, then shows little variation from $n=6-25$. This abrupt transition suggests that the nature of the electron-solvent interaction changes around $n=6$. Hence, for this and larger clusters, the single observed feature is relabeled as feature A′.

Varying the ion source conditions by adjusting the argon backing pressure from 20–35 psig does not change the photoelectron spectra for the $n=1$ and $n=26$ anions, suggesting that there are no other markedly different binding motifs (isomers) of the solvent cluster anions over this size range.

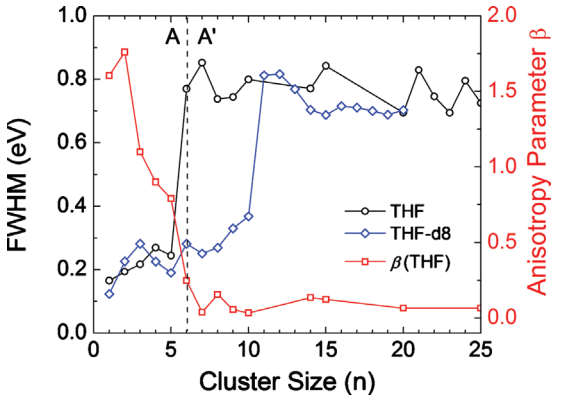

FIG. 4. FWHM and photoelectron anisotropy parameter (β) as a function of cluster size for the $n \leq 25$. The change in the photoelectron angular distribution occurs at the same cluster size as the drastic change in the width of the spectrum from feature A to feature A′ at $n=6$. A dashed line is drawn through $n=6$ to highlight the change.

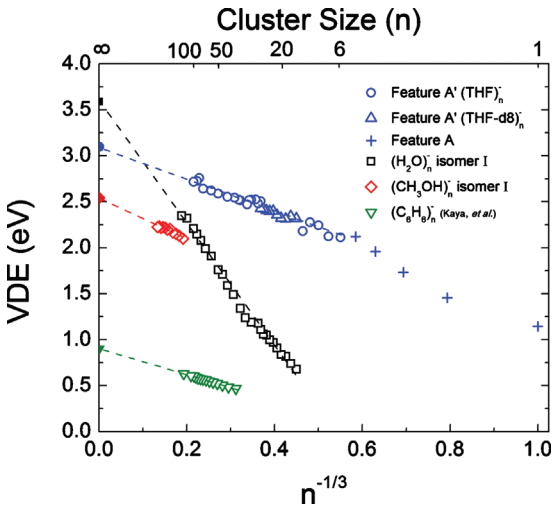

FIG. 5. VDEs of feature A′ $(THF)_n^-$, $n \geq 6$ (open blue circles) and $(THF\text{-}d8)_n^-$, $n \geq 11$ (open blue triangles) are shown, along with those of $(C_6H_6)_n^-$ [adapted from Mitsui, *et al.* (Ref. 17)] and isomer I of $(CH_3OH)_n^-$ [open red diamonds, which are adapted from Kammrath, *et al.* (Ref. 18)] and $(H_2O)_n^-$ [open black squares, adapted from Kammrath, *et al.* (Ref. 48)] vs $n^{-1/3}$. Linear fits are superposed upon their respective data, projected out to $n=\infty$ (solid markers). VDEs for feature A for $(THF)_n^-$, $n<6$ (blue crosses) are also shown.

Examination of the deuterated clusters $(THF\text{-}d8)_n^-$ at an Ar backing pressure of 20 psig shows similar trends with a few important differences. Feature A is present, but is significantly less intense relative to feature B in small clusters, as shown in Fig. 2 for $n=1$. Moreover, the shape of feature A does not change until $n=11$, at which point the abrupt transition analogous to that seen in THF occurs (see Fig. 4). For $n \geq 11$, the VDEs of $(THF\text{-}d8)_n^-$ clusters are identical to those in Fig. 3.

IV. DISCUSSION

In this section, we examine the photoelectron spectra in detail, focusing first on the larger size regime beyond the transition to feature A′. The measured VDEs in this size regime are compared to those of other solvated electron clusters. These results are also considered within the context of dielectric continuum theory. We then consider the smaller clusters and the possible origins of features A and B. Finally, we speculate on the structure of THF clusters with excess electrons.

A. Large clusters

The PE spectra of the anion clusters with $n \geq 6$ comprise a single feature A′, which undergoes only gradual changes with increasing cluster size. More specifically, this feature is very broad (FWHM=0.77 eV for $n=6$, and 1.04 eV for $n=100$), its shape is relatively constant with cluster size over the size range of $n=6-100$, and it shifts only gradually toward higher VDE with increasing cluster size. Figure 5 shows that a plot of the feature A′ VDEs as a function of $n^{-1/3}$ yields a straight line, as it does for the VDEs of $(C_6H_6)_n^-$ clusters[17] and isomer I of $(H_2O)_n^-$ and $(CH_3OH)_n^-$ clusters,[11,18,48] all of which are shown in the figure. These attributes of feature A′ are characteristic of solvated electron clusters, in which the excess electron is bound to multiple intact solvent molecules.[22,49] Hence, we assign feature A′ to $(THF)_n^-$ clusters, in which the excess electron is solvated by intact THF molecules.

Comparison among the solvating species in Fig. 5 indicates several notable trends. First, the VDEs for $(THF)_n^-$ clusters are noticeably higher than those for other solvated electron clusters in the same size regime even for isomer I water cluster anions. Second, the minimum size at which an assignable THF solvated electron cluster is identified is comparable to that of water but much smaller than for benzene ($n=53$) and methanol ($n=143$ for isomer I, $n=70$ for the more weakly bound isomer II). The slope of the VDEs for $(THF)_n^-$ clusters in Fig. 5 is comparable to that for methanol and benzene cluster anions but considerably less than that for water cluster anions. Finally, the value of the y-intercept is of considerable interest, since it should, in principle, yield the binding energy of the electron in the bulk solvent. The validity of this extrapolation has recently been demonstrated for water cluster anions through measurement of the VDE of hydrated electrons in liquid water microjets,[50–52] which yield values ranging from 3.3 to 3.6 eV. Figure 5 implies that a similar measurement for THF would yield 3.10 eV.

The linear variation of the VDEs versus $n^{-1/3}$ is predicted by dielectric continuum (DC) theory,[53,54] which is an appropriate first approximation for the energetics of solvated electron clusters. If it is assumed that the electron resides inside a spherical cluster consisting of a uniform dielectric material, DC theory finds that

$$\mathrm{VDE}(n) = \mathrm{VDE}(\infty) - \frac{e^2}{8\pi\varepsilon_0 r_0}\left(1 + \frac{1}{\varepsilon_\infty} - \frac{2}{\varepsilon_s}\right)n^{-1/3}, \quad (3)$$

$$\mathrm{VDE}(\infty) = \frac{e^2}{8\pi\varepsilon_0 a_0}\left(1 + \frac{1}{\varepsilon_\infty} - \frac{2}{\varepsilon_s}\right). \quad (4)$$

Here n is the cluster size, VDE(∞) is the bulk photoelectric threshold, r_0 is the average molecular radius, a_0 is the bulk cavity radius for the solvated electron, ε_0 is the permittivity of free space, and ε_∞ and ε_s are the optical and static dielectric constants, respectively. Moment analysis of the solvated

TABLE I. Dielectric continuum (DC) theory values. The temperatures represent bounds for that of our anion beam.

	150 K	200 K	Expt.
r_0 (Å)[a]	3.03	3.08	
a_0 (Å)[b]	3.46	3.86	
ε_∞ [c]	2.201	2.128	
ε_s [d]	16.17	11.75	
eBE(∞) (eV)	2.77	2.42	3.10 ± 0.03
Slope (eV)	−3.16	−3.04	-1.74 ± 0.09

[a]Reference 57.
[b]References 55 and 56.
[c]Reference 58.
[d]Reference 59.

electron absorption spectrum of THF is used to estimate the cavity radius of the electron.[55,56] The molecular radius is estimated from the molar volume of liquid THF,[57] and the optical dielectric constant is taken to be the square of the refractive index.[58] The temperature dependence of these values, as well as that of the static dielectric constant[59] has been accounted for by using two temperatures which should bracket that of $(THF)_n^-$ clusters in our ion beam. Values and results are summarized in Table I.

The experimental VDEs show qualitative agreement with the DC model, as they scale linearly with the radius of the cluster ($\sim n^{-1/3}$), with a slope of -1.74 ± 0.09 eV and an intercept of $+3.10 \pm 0.03$ eV. The disagreement between the experimental and predicted values for the slope and intercept highlights the simplicity of this model, which neglects molecularity and the disorder associated with solvent packing. For example, the effective molecular radius necessary to yield the experimental value for the slope would be 4.8 Å, which is larger than the experimentally determined electron cavity radius of ~4 Å in bulk THF.[55]

As noted previously,[11,17,18] DC theory reproduces the experimental slopes and intercepts for water and benzene quite well with little or no adjustment of the input parameters, but predicts a considerably larger slope for methanol, 4.3 eV versus the experimental value of 2.25 eV for $(CH_3OH)_n^-$ clusters. The agreement between experiment and DC theory is better for THF than for methanol, but not as good as for water or benzene. It is not entirely surprising that a purely electrostatic model such as DC theory does not yield quantitative agreement for electrons in THF, given the complexity of the neat solvent and its interactions with solvated electrons.[30,36]

B. Small anions

We next consider the PE spectra for anions with masses corresponding to $(THF)_n^-$, $n=1-5$. The PE spectrum of $m/z=72$ (Fig. 2) deserves special attention. Although this mass nominally corresponds to THF^-, THF has a has a closed-shell electronic configuration and a large HOMO-LUMO gap,[60,61] so a thermodynamically stable anion with the excess electron residing in a valence orbital is unlikely. The dipole moment of THF in the gas phase is between 1.64 (Ref. 62) and 1.75 D.[63] These values lie just above the minimum dipole moment of 1.62 D needed to support a anionic dipole-bound state,[64] but such states are typically bound by ~10–100 meV,[65–68] much less than the VDE of either feature A or B. Our computational investigations have revealed no valence-bound states for THF anion geometries starting from the C_1, C_2, or C_s symmetries. However, higher-level treatments may be necessary to fully characterize a valence-bound THF anion theoretically.

TABLE II. Calculated vertical detachment energies for the butoxyl anion (eV).

Hydride shifts	Anion structure	Neutral spin multiplicity	
		Singlet	Triplet
0		2.728	2.087
1	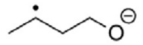	1.823	2.220
2	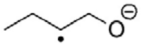	1.901	1.978

To the best of our knowledge, the only observation of an anion with the mass of THF is from an electron scattering experiment by Sulzer *et al.*[26] A weak negative ion signal of mass 72 was observed upon bombardment of THF in an effusive molecular beam with 1.25 eV electrons. Since parent ions formed by electron attachment to isolated molecules are generally unstable with respect to dissociation or autodetachment, this signal was attributed to a metastable anion of unknown structure. Subsequent electron scattering studies on THF by Ibanescu *et al.*[27] did not reveal negative ion signal at $m/z=72$; only smaller anion fragments formed by dissociative electron attachment were observed starting at electron energies of 6 eV. It is possible that the parent ion signal seen by Sulzer *et al.*[26] came from low energy dissociative attachment to a THF cluster. Such a process is likely to occur in our ion source as well, given the relatively high concentration of neutral clusters produced in a pulsed molecular beam.

Focusing next on the anion structures associated with features A and B in the anion PE spectrum in Fig. 2, we note that the PE spectrum of feature B is very similar to that of the anion with $m/z=71$ which, as mentioned above, is the open-chain *sec*-butyraldehyde enolate anion $[(1,2)\text{-}s\text{-}C_4H_7O^-]$ previously observed by Continetti *et al.*[47] This species is presumably formed in the ion source by electron-induced opening of the ether ring and proton loss. It is therefore reasonable to explore whether feature B with $m/z=72$ is an open chain radical isomer of $C_4H_8O^-$. The most stable such isomer is expected to be the butoxyl radical anion, with the excess electron localized on the oxygen atom. Similar structures have comparable binding energies to that of feature B (1.87 eV), such as the *tert*-butoxyl radical, 1.91 eV,[69] and the neopentoxyl radical, 1.93 eV.[70]

There are several candidate structures for the butoxyl anion radical structure that can be evaluated because the sigmatropic hydride shifting along the carbon chain causes significant changes in the VDE. DFT calculations are used to determine which radical species may give rise to the observed peaks in the spectra; the results of these calculations are shown in Table II. The VDEs of the lower two structures

are very similar to one another and to that of feature B. We thus attribute feature B at $m/z=72$ to a radical anion of this kind that has undergone at least one hydride shift, detaching to a neutral C_4H_8O diradical in its singlet state. The structure with the radical center on the carbon alpha to the oxygen atom cannot be treated accurately with DFT, as geometry optimizations of the anion leads to unphysical structures and a negative vertical detachment energy. As deuteration does not affect electronic states, the analogous species is also the likely source of feature B in the THF-d8 spectra. The shift in feature B toward higher VDE in the $n=2-5$ PE spectra is then consistent with this ion being progressively solvated[71] until it is bound by more than the photon energy (3.14 eV) by $n=6$.

The origin of feature A is more difficult to ascertain. Although the VDE is lower than that of feature B, it is still too large to be from a dipole-bound state. Feature A could be from another open-shell anion structure that we were unable to locate by electronic structure calculations. However, this seems unlikely because as additional solvent molecules are added, its VDE evolves smoothly into that of feature A′ for the larger clusters. In fact, as shown in Fig. 5, the VDEs for feature A over the entire size range $n=1-5$ lie quite close to the straight line determined by the VDEs of the clusters with $n\geq 6$. Hence, although feature A is quite distinct from feature A′ in terms of its width and photoelectron angular distribution (Fig. 4), it appears to arise from some type of anion structure that maps onto the solvated electron clusters with increasing size.

There is no evidence that an intact THF ring has a positive adiabatic electron affinity. It is possible, however, that a distorted ring can bind an electron, leading to a long-lived negative ion with a positive vertical detachment energy through stabilization of the lowest unoccupied molecular orbital (LUMO) in THF. Such a distorted structure could serves as the electron binding site in the anions with $n=1-5$, resulting in feature A upon photodetachment. The CO_2 and N_2O molecules are well known examples of this phenomenon. Neither molecule exhibits a positive adiabatic electron affinity,[72] but in both cases, the LUMO is stabilized by bending to the extent that bent CO_2^- and N_2O^- anion have been observed in mass spectrometry and photoelectron spectroscopy experiments.[73–75] These anions have positive VDEs (~1 eV) and live long enough for their photoelectron spectra to be measured. Moreover, the VDEs of the bare anions increase upon addition of additional solvent molecules, as is the case with feature A. The HOMO-LUMO gap in THF is similar to that in CO_2 and N_2O [7.29 eV (Ref. 76) and 6.52 eV,[77] respectively, compared to 6.29 eV (Ref. 60) for THF], so a similar extent of stabilization induced by distortion is needed to bind an electron to THF. However, the PE spectra of bare and solvated CO_2^- and N_2O^- are about 0.7 eV wide, much broader than that of feature A in the THF anion PE spectra, so it remains to be seen whether this analogy is plausible.

C. General remarks

THF is a widely used solvent for studying electron dynamics in the condensed phase. It is weakly polar, having a relatively low dielectric constant ($\varepsilon_s=7.33$ at room temperature), which makes it a versatile solvent. Additionally, its large spectral transmission window makes it very convenient for optical spectroscopy, particularly in the case of the solvated electron, which in THF absorbs intensely in the infrared. The electron is not known to interact strongly with one or a small number of THF molecules directly, only associating with the collective dipole moments of those immediately surrounding it,[30] making it a true "solvated" electron. The formation of a stable or metastable THF^- anion would complicate this picture, particularly if this species can exist alongside the solvated electron. Prior to this study, it was not known if THF clusters could support an excess electron at all. However, the high value of the VDE of solvated electron state in THF at onset, higher than that of any comparably sized solvent clusters studied thus far, suggests that the electron is highly stabilized, even for very small clusters.

As in the bulk, preexisting electropositive voids within the clusters can act as natural traps for electron attachment, requiring little solvent reorganization to accommodate the excess charge. The relative agreement with the bulk values for even small clusters, which lie on the same line as those near $n=100$, suggests that this feature of the bulk solvent structure might facilitate electron solvation in THF clusters. By contrast, neat liquid water does not exhibit these polarized cavities, and the injection of an electron requires the water network to reorder around it. Thus one would expect the binding energies in the anionic clusters to be smaller, and change more rapidly than those for clusters which naturally form these structures. Hydrogen-bonding interactions should be almost entirely absent in THF solution and clusters, so there is no strong bonding network that must be disrupted in order to accommodate an excess electron internally. The liquid structure of THF is influenced by the formation of T-shaped pairings of the ether rings,[36] evocative of the benzene dimer in the gas phase.[78]

The absence of other isomers for the electron at these sizes for different source conditions differs from water and methanol cluster anions,[18,79] where colder conditions (higher backing pressures) were shown to produce anions with lower binding energies, attributed to surface-bound electron states. In THF, the presence of nascent voids could explain the lack of observation of a surface-bound state, as it would create a porous network with multiple, deep potential energy wells accessible to the electron, allowing for internal solvation. This suggests that the electrons are internally solvated within these clusters. It is interesting to note that the disklike THF molecules could form a closed, hollow structure with as few as six molecules in a quasicubic arrangement. It would clearly be of interest to perform electron structure calculations on small THF anion clusters in order to gain a firmer understanding of the experimental trends observed here.

V. CONCLUSION

We have measured photoelectron spectra of size-selected tetrahydrofuran cluster anions up to $n=100$ at $h\nu=3.14$ eV. This study represents the first observation and characterization of $(THF)_n^-$ clusters. The PE spectra of clusters with n

$=1-5$ exhibit two sharp peaks, features A and B, which are attributed to an anion of the unopened THF ring and an open-chain butoxyl radical anion, respectively. PE spectra for clusters with $n \geq 6$ show a single broad peak, feature A′. The size dependence of this feature exhibits characteristics of a cluster-solvated electron. With the THF cluster energetics established, we hope to investigate the time-resolved solvated electron dynamics analogous to our previous water[13] and methanol[19] work, as well as investigate the CTTS dynamics in the gas-phase to draw a direct comparison to the work done on the dynamics in the condensed phase.[80] Liquid jet measurements on the bulk solvated electron in THF will also be of use and will soon be underway in our laboratory.

ACKNOWLEDGMENTS

This work was supported by the National Science Foundation (CHE-0649647). R.M.Y. is grateful to the Samuel Ruben/Irv Fatt Fellowship, and M.A.Y. was supported by DoD, Air Force Office of Scientific Research, National Defense Science and Engineering Graduate (NDSEG) Fellowship, 32 CFR 168a. The authors are also grateful to Tara Yacovitch for her help with the *ab initio* calculations, and to Dr. Oli Ehrler for his advice and assistance in building our new data acquisition program.

[1] J. Schnitker and P. Rossky, J. Chem. Phys. **86**, 3471 (1987).
[2] M. Boero, M. Parrinello, K. Terakura, T. Ikeshoji, and C. C. Liew, Phys. Rev. Lett. **90**, 226403 (2003).
[3] F. Arnold, Nature (London) **294**, 732 (1981).
[4] J. Simons, Acc. Chem. Res. **39**, 772 (2006).
[5] H. F. Hameka, G. W. Robinson, and C. J. Marsden, J. Phys. Chem. **91**, 3150 (1987).
[6] R. E. Larsen, W. J. Glover, and B. J. Schwartz, Science **329**, 65 (2010).
[7] E. J. Hart and M. Anbar, *The Hydrated Electron* (Wiley-Interscience, New York, 1970).
[8] W. Weyl, Ann. Phys. **199**, 350 (1864).
[9] G. R. Freeman, J. Chem. Phys. **77**, 7 (1973).
[10] J.-P. Jay-Gerin and C. Ferradin, Radiat. Phys. Chem. **36**, 317 (1989).
[11] J. V. Coe, G. H. Lee, J. G. Eaton, S. T. Arnold, H. W. Sarkas, K. H. Bowen, C. Ludewigt, H. Haberland, and D. R. Worsnop, J. Chem. Phys. **92**, 3980 (1990).
[12] P. Ayotte and M. A. Johnson, J. Chem. Phys. **106**, 811 (1997).
[13] G. B. Griffin, R. M. Young, O. T. Ehrler, and D. M. Neumark, J. Chem. Phys. **131**, 194302 (2009).
[14] L. Ma, K. Majer, F. Chirot, and B. v. Issendorff, J. Chem. Phys. **131**, 144303 (2009).
[15] M. Mitsui, N. Ando, S. Kokubo, A. Nakajima, and K. Kaya, Phys. Rev. Lett. **91**, 153002 (2003).
[16] R. M. Young, G. B. Griffin, A. Kammrath, O. T. Ehrler, and D. M. Neumark, Chem. Phys. Lett. **485**, 59 (2010).
[17] M. Mitsui, A. Nakajimaa, and K. Kaya, J. Chem. Phys. **117**, 9740 (2002).
[18] A. Kammrath, J. R. R. Verlet, G. B. Griffin, and D. M. Neumark, J. Chem. Phys. **125**, 171102 (2006).
[19] A. Kammrath, G. B. Griffin, J. R. R. Verlet, R. M. Young, and D. M. Neumark, J. Chem. Phys. **126**, 244306 (2007).
[20] T. Maeyama, Y. Negishi, T. Tsukuda, I. Yagia, and N. Mikami, Phys. Chem. Chem. Phys. **8**, 827 (2006).
[21] J. V. Coe, Int. Rev. Phys. Chem. **20**, 33 (2001).
[22] D. M. Neumark, Mol. Phys. **106**, 2183 (2008).
[23] M. Allan, J. Phys. B **40**, 3531 (2007).
[24] C. S. Trevisan, A. E. Orel, and T. N. Rescigno, J. Phys. B **39**, L255 (2006).
[25] S. Tonzani and C. H. Greene, J. Chem. Phys. **125**, 094504 (2006).
[26] P. Sulzer, S. Ptasinska, F. Zappa, B. Mielewska, A. R. Milosavljevic, P. Scheier, T. D. Märk, I. Bald, S. Gohlke, M. A. Huels, and E. Illenbergere, J. Chem. Phys. **125**, 044304 (2006).
[27] B. C. Ibănescu, O. May, and M. Allan, Phys. Chem. Chem. Phys. **10**, 1507 (2008).
[28] D. Duflot, J.-P. Flament, J. Heinesch, and M.-J. Hubin-Franskin, Chem. Phys. Lett. **495**, 27 (2010).
[29] E. R. Barthel, I. B. Martini, and B. J. Schwartz, J. Chem. Phys. **112**, 9433 (2000).
[30] M. J. Bedard-Hearn, R. E. Larsen, and B. J. Schwartz, J. Chem. Phys. **122**, 134506 (2005).
[31] M. J. Bedard-Hearn, R. E. Larsen, and B. J. Schwartz, J. Chem. Phys. **125**, 194509 (2006).
[32] M. C. Cavanagh, R. M. Young, and B. J. Schwartz, J. Chem. Phys. **129**, 134503 (2008).
[33] A. E. Bragg, M. C. Cavanagh, and B. J. Schwartz, Science **321**, 1817 (2008).
[34] O. Shoshana, J. L. P. Lustres, N. P. Ernsting, and S. Ruhman, Phys. Chem. Chem. Phys. **8**, 2599 (2006).
[35] X. Chen and S. E. Bradforth, Annu. Rev. Phys. Chem. **59**, 203 (2008).
[36] D. T. Bowron, J. L. Finney, and A. K. Soper, J. Am. Chem. Soc. **128**, 5119 (2006).
[37] Y. S. Park, H. Cho, L. Parenteau, A. D. Bass, and L. Sanche, J. Chem. Phys. **125**, 074714 (2006).
[38] A. V. Davis, R. Wester, A. E. Bragg, and D. M. Neumark, J. Chem. Phys. **118**, 999 (2003).
[39] U. Even, J. Jortner, D. Noy, N. Lavie, and C. Cossart-Magos, J. Chem. Phys. **112**, 8068 (2000).
[40] W. C. Wiley and I. H. McLaren, Rev. Sci. Instrum. **26**, 1150 (1955).
[41] A. T. J. B. Eppink and D. H. Parker, Rev. Sci. Instrum. **68**, 3477 (1997).
[42] V. Dribinski, A. Ossadtchi, V. A. Mandelshtam, and H. Reisler, Rev. Sci. Instrum. **73**, 2634 (2002).
[43] M. J. Travers, D. C. Cowles, and G. B. Ellison, Chem. Phys. Lett. **164**, 449 (1989).
[44] K. L. Reid, Annu. Rev. Phys. Chem. **54**, 397 (2003).
[45] J. Cooper and R. N. Zare, J. Chem. Phys. **48**, 942 (1968).
[46] M. J. Frisch, G. W. Trucks, H. B. Schlegel *et al.*, GAUSSIAN 03, Gaussian, Inc., Wallingford, CT, 2004.
[47] L. S. Alconcel, H.-J. r. Deyerl, and R. E. Continetti, J. Am. Chem. Soc. **123**, 12675 (2001).
[48] A. Kammrath, J. R. R. Verlet, G. B. Griffin, and D. M. Neumark, J. Chem. Phys. **125**, 076101 (2006).
[49] J. V. Coe, S. M. Williams, and K. H. Bowen, Int. Rev. Phys. Chem. **27**, 27 (2008).
[50] K. R. Siefermann, Y. X. Liu, E. Lugovoy, O. Link, M. Faubel, U. Buck, B. Winter, and B. Abel, Nat. Chem. **2**, 274 (2010).
[51] Y. Tang, H. Shen, K. Sekiguchi, N. Kurahashi, T. Mizuno, Y. I. Suzuki, and T. Suzuki, Phys. Chem. Chem. Phys. **12**, 3653 (2010).
[52] A. T. Shreve, T. A. Yen, and D. M. Neumark, Chem. Phys. Lett. **493**, 216 (2010).
[53] R. N. Barnett, U. Landman, and C. L. Cleveland, Chem. Phys. Lett. **145**, 382 (1988).
[54] X.-J. Wang, Q. Zhu, Y.-K. Li, X.-M. Cheng, X.-Y. Li, K.-X. Fu, and F.-C. He, J. Phys. Chem. B **114**, 2189 (2010).
[55] F.-Y. Jou and G. R. Freeman, Can. J. Chem. **54**, 3693 (1976).
[56] W. Marbach, A. N. Asaad, and P. Krebs, J. Phys. Chem. A **103**, 28 (1999).
[57] R. P. W. Scott and J. Liq, Chromatogr. R. T. **23**, 3083 (2000).
[58] G. Openhaim and E. Grushka, J. Chromatogr. A **942**, 63 (2002).
[59] D. J. Metz and A. Clines, J. Phys. Chem. **71**, 1158 (1967).
[60] L. W. Pickett, N. J. Hoeflich, and T.-C. Liue, J. Am. Chem. Soc. **73**, 4865 (1951).
[61] P. Duffy, A. Sordo, and F. Wang, J. Chem. Phys. **128**, 125102 (2008).
[62] D. D. Klug and E. Whalle, Can. J. Chem. **51**, 4062 (1973).
[63] D. R. Lide, in *CRC Handbook of Chemistry and Physics*, edited by D. R. Lide (CRC/Taylor & Francis, Boca Raton, FL/London, 2010), p. 50.
[64] J. A. D. Stockdale, L. G. Christophorou, J. E. Turner, and V. E. Anderson, Phys. Lett. **25A**, 510 (1967).
[65] S. Y. Han, J. H. Kim, J. K. Song, and S. K. Kim, J. Chem. Phys. **109**, 9656 (1998).
[66] K. R. Lykke, R. D. Mead, and W. C. Lineberger, Phys. Rev. Lett. **52**, 2221 (1984).
[67] J. H. Hendricks, S. A. Lyapustina, H. L. deClercq, and K. H. Bowen, J. Chem. Phys. **108**, 8 (1998).
[68] N. I. Hammer, K. Diri, K. D. Jordan, C. Desfrancois, and R. N. Compton, J. Chem. Phys. **119**, 3650 (2003).
[69] T. M. Ramond, G. E. Davico, R. L. Schwartz, and W. C. Lineberger, J.

Chem. Phys. **112**, 1158 (2000).
[70] P. S. Drzaic, J. Marks, and J. I. Brauman, in *Gas Phase Ion Chemistry*, edited by M. T. Bowers (Academic, Orlando, FL, 1984), Vol. 3, p. 167.
[71] A. W. Castleman, Jr., and K. H. Bowen, Jr., J. Phys. Chem. **100**, 12911 (1996).
[72] S. T. Arnold, J. V. Coe, J. G. Eaton, C. B. Freidhoff, L. H. Kidder, G. H. Lee, M. R. Manaa, K. M. McHugh, D. Patel-Misra, H. W. Sarkas, J. T. Snodgrass, and K. H. Bowen, in *Proceedings of the Enrico Fermi International School of Physics*, CVII Course, Varenna, edited by G. Scoles (North Holland, Amsterdam, 1989), pp. 467.
[73] C. D. Cooper and R. N. Compton, Chem. Phys. Lett. **14**, 29 (1972).
[74] J. V. Coe, Ph.D. thesis, The Johns Hopkins University, 1986.
[75] J. V. Coe, J. T. Snodgrass, C. B. Freidhoff, K. M. McHugh, and K. H. Bowen, Chem. Phys. Lett. **124**, 274 (1986).
[76] K. Yoshino, J. R. Esmond, Y. Sun, W. H. Parkinson, K. Ito, and T. Matsui, J. Quant. Spectrosc. Radiat. Transf. **55**, 53 (1996).
[77] G. Selwyn, J. Podolske, and H. S. Johnston, Geophys. Res. Lett. **4**, 427 (1977).
[78] K. C. Janda, J. C. Hemminger, J. S. Winn, S. E. Novick, S. J. Harris, and W. Klemperer, J. Chem. Phys. **63**, 1419 (1975).
[79] J. R. R. Verlet, A. E. Bragg, A. Kammrath, O. Cheshnovsky, and D. M. Neumark, Science **307**, 93 (2005).
[80] A. E. Bragg and B. J. Schwartz, J. Phys. Chem. B **112**, 483 (2008).